COBEM 2021 Florianópolis - Brasil
26th ABCM International Congress of Mechanical Engineering
November 22-26, 2021. Florianópolis, SC, Brazil

COB-2021-0931
EXERGY ANALYSIS OF A SOLAR-BIOMASS HYBRID COGENERATION POWER PLANT APPLIED TO CORN ETHANOL PRODUCTION IN BRAZIL AND THE UNITED STATES

Lauro Augusto J. Oliveira
Edson Bazzo
Federal University of Santa Catarina, Department of Mechanical Engineering, LabCET – Combustion and Thermal Systems Engineering Laboratory, Florianópolis - SC - Brazil
lauro.oliveira@labcet.ufsc.br, e.bazzo@ufsc.br

Eduardo K. Burin
Federal University of Paraná, Department of Engineering and Exact Sciences, Palotina - PR - Brazil
eduardo.burin@ufpr.br

Abstract. *This study compares the energy and exergy performance of a concentrated solar power (CSP) and biomass hybridized corn ethanol cogeneration cycle located in the United States (Phoenix/AZ) and Brazil (Barreiras/BA). The proposed hybrid plant uses in parallel a biomass boiler and a direct steam generation parabolic trough solar field to supply a 28.5 MW backpressure steam turbine with about 49 kg/s of superheated steam at 520 °C and 67 bar. After the turbine, steam at saturated state supply process heat to a dried distillery grain with solubles (DDGS) dryer, at 9 bar and 12.5 kg/s, and the ethanol production processes, at 2.5 bar and 37.5 kg/s. The plant operates on a fuel-saving strategy, meaning that the boiler and solar field supply the plant's steam requirement at all times. For each location, the solar field size is determined following the criteria that the concentrators deliver a maximum of 60% of the steam generation for design DNI and larger irradiance levels. The biomass is eucalyptus wood chips with 30 % of moisture content. The analyzed performance indicators are the annual energy and exergy efficiencies, the economized fuel, the destroyed exergy, and the biomass savings. These indicators are calculated for the design-point conditions and the typical meteorological year. Ebsilon Professional is the computational tool used for the performance assessment, while the meteorological data comes from the software Meteonorm. The study results show the technical feasibility of the proposed solution for both locations but with an advantage for Barreiras.*

Keywords: *Concentrated solar power, Corn ethanol production, Direct steam generation, Solar-biomass hybrid cogeneration*

1. INTRODUCTION

Bioethanol has a relevant role in the future of the different energy matrixes worldwide as a sustainable non-fossil fuel and energy carrier. By far, the leading producers of bioethanol are the USA and Brazil. According to the Renewable Fuel Association (RFA, 2019), in 2018, the first country accounted for 56% of global ethanol production while the second country 28%. However, the American and Brazilian ethanol industries achieve their global production shares in different ways. While the United States produces ethanol using corn as feedstock, until recently, Brazil focused on producing ethanol solely from sugarcane, given historical and technological developments of the industry in the country.

Nonetheless, in the past few years, as corn production rose in Brazil's Central-West region, the price of corn fell to levels that allowed for the sprouting of a corn ethanol industry. The first attempts to produce ethanol from corn in Brazil started by adapting sugar cane mills to produce corn ethanol in off-season periods in the so-called flex-fuel mills. Later came the plants that process only corn (Eckert et al., 2018).

Ethanol plants consume a large amount of electricity and process heat to function. Therefore, cogeneration, also known as combined heat and power (CHP), can provide a more efficient energy supply. For example, a typical corn ethanol plant in the US utilizes around 9.7 MJ of process heat and 0.29 kWh of electricity per liter of ethanol produced (Mani et al., 2010). These energy consumption values are, in general, lower than those present in sugarcane ethanol plants. However, when looking at the primary energy source used, there is a relevant difference between ethanol production from corn and sugarcane. While sugarcane plants burn the bagasse obtained by processing its feedstock, corn ethanol plants need to use external fuel sources such as fossil fuels or wood chips, increasing their operation costs (Nogueira et al., 2014).

Researchers have proposed various ways to mitigate corn ethanol plants' demand for external fuel sources. Karuppiah et al. (2008) focused on plant design, optimizing thermochemical processes to reduce overall energy requirements. Morey

et al. (2006), Tiffany et al. (2008), and Wang et al. (2009) examined the viability of burning co-products such as Dried Distillery Grains with Solubles (DDGS) and corn stover as boiler fuel. Kam et al. (2009) also examined the possibility of using DDGS and corn stover as fuel by comparing their direct combustion and their gasification for subsequent firing. Another possible way to remedy the corn ethanol plant's energy supply is to associate concentrated solar energy with the cogeneration cycle. Among the different CSP technologies, Parabolic Trough Collectors (PTC) stand out as the most mature CSP technology and the most optically efficient linear collectors. PTC concentrators are typically used for indirect heat generation. In this configuration, synthetic oils are used as working fluids that carry the heat acquired in the concentrators to the steam cycle through a heat exchanger at a maximum temperature of 400 °C (Fuqiang et al., 2017). The concept of indirect heating using PTC was considered to the corn ethanol industry by Brunet et al. (2014) in a study focused on distillation tower heating. Alternatively, PTC can also operate in Direct Steam Generation (DSG), heating water directly and generating steam with temperatures up to 500 °C (Giglio et al., 2017). A third CSP application possibility would be to preheat feed water. For example, Burin et al. (2015) studied this concept in the sugar cane ethanol industry. Finally, no studies were found regarding corn ethanol plants using CSP solar fields to generate steam directly. Energy and exergy analyses are alternatives to evaluate the performance of these new corn ethanol plant arrangements. In this regard, for example, Donke et al. (2013) reported an energo and exergo-environmental study of typical sugarcane, corn, and flex-mill ethanol plants. They concluded that the corn ethanol plant with cogeneration would be the scenario that presents the most balanced energetic, exergetic, and environmental performance. López et al. (2018) performed the exergy analysis of a sugarcane bagasse ethanol plant assisted by linear Fresnel concentrators. The solar field was analyzed in two configurations: a feedwater preheater before the boilers and a heater that delivers saturated steam. The first configuration performed better, resulting in 10% fuel saving and a reduction of 11% of overall exergy destruction.

Given the outlined scenario, this paper presents the energy and exergy performance evaluation of a hybrid solar-biomass cogeneration cycle for a typical corn ethanol plant. The assessment is made for two plant locations: Pheonix/AZ (USA) and Barreiras/BA (Brazil). The analyzed hybrid plant uses a parabolic trough solar field under direct steam generation in parallel to a biomass boiler to meet the plant's steam requirements. The analysis evaluates the biomass savings, the plant's energy efficiencies, the destroyed exergy and the exergy efficiencies for the design point condition, and a typical meteorological year (TMY), in each plant location.

2. METHODOLOGY

2.1 Cogeneration cycle description

As seen in Figure 1, the proposed hybrid cogeneration cycle is composed of a typical corn ethanol base cycle, as described by surveyed Brazilian engineering companies, and a parabolic trough concentrator solar field. The typical plant modeled produces 800 m^3 of ethanol per day (292,000 m^3/year). For this level of ethanol production, the boiler and the solar field need to generate 48.4 kg/s of superheated steam together at 520 °C and 67 bar to power the plant's 28,5 MW Back Pressure Steam Turbine (BSPT). From the turbine, 12.5 kg/s of steam is extracted at 11 bar to feed the DDGS dryer. Here a pressure drop of 2 bar was considered for analysis.

Further on, at the turbine's exhaust, 37.5 kg/s of steam is discharged at 4.5 bar to feed the deaerator at 2 bar, and the ethanol production processes at 2.5 bar. After the production processes, the condensate is directed to a condensate tank, at atmospheric pressure, where flash steam is eliminated, and make-up water is supplied at 25 °C. The condensate is then pumped to the deaerator from which it leaves to be pumped back to the boiler and solar field at 77 bar and the water injectors (desuperheaters) at 9 bar. All pressures are considered absolute.

The biomass used in the boiler is eucalyptus wood chips, with corresponding elemental composition and low heating value available in Table 1. The solar field is composed of Eurotrough ET-150 concentrators in a once-through configuration. The steam cycle's design parameters can be found in Table 2 and Table 3. The plant follows the fuel-saving operation strategy in which the sum of the steam generated by the boiler and solar field is equal to the plant's nominal steam requirement. Thus, at its design point, the solar field produces 60% of the steam required to feed the cogeneration cycle while the boiler operates at its minimum load of 40%.

Table 1. Eucalyptus biomass elemental composition in wet basis and low heating value

Parameter	C (%)	H (%)	O (%)	N (%)	Ash (%)	Moisture (%)	LHV (kJ/kg)[(1)]
Value	35.00	4.67	29.40	0.11	0.82	30.00	12747

[(1)] Calculated by the Mendeleev formula as described in Cortez et al. (2008).

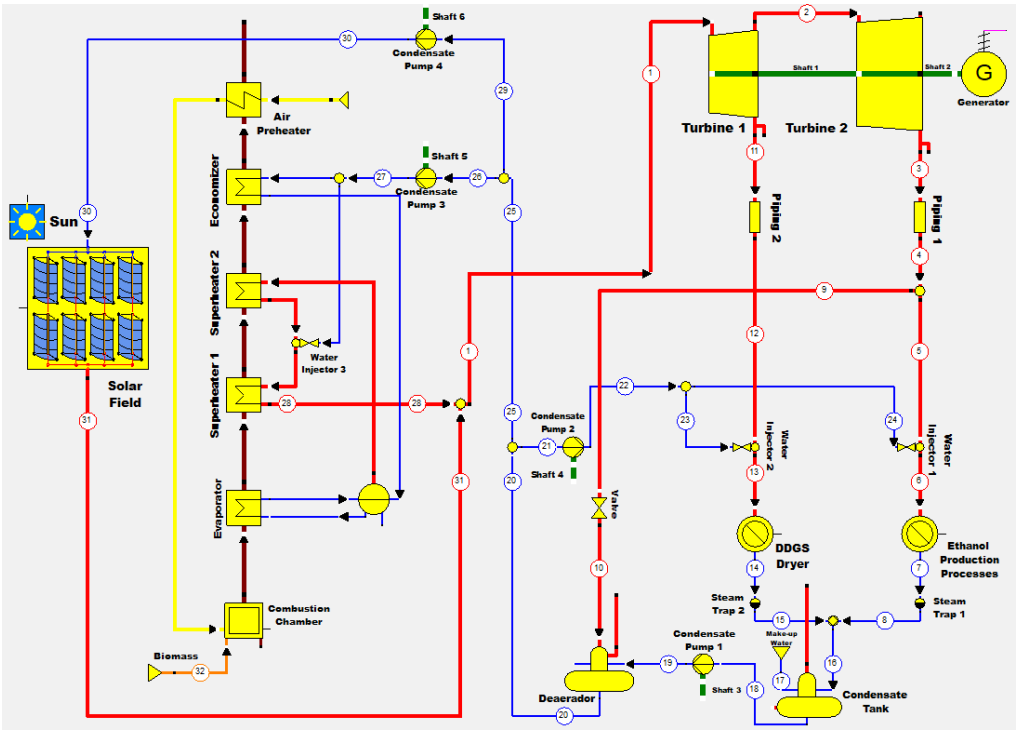

Fig. 1. Modeled solar-biomass hybrid cogeneration cycle's schematic

Table 2. Plant design parameters

Parameters	Value
Boiler	
Steam pressure, bar	67
Steam temperature, °C	520
Global heat transfer coefficients, kWm^2/K	
Evaporator	99
Superheater 1	70
Superheater 2	13
Economizer	41
Air preheater	290
Combustion chamber efficiency, %	99
Excess air(1), %	50
Boiler slag temperature, °C	400
Fly ash ratio, %	30
Wall heat transfer losses(2), %	2
Power block	
Turbine 1 isentropic efficiency, %	85
Turbine 2 isentropic efficiency, %	88
Pumps isentropic efficiency, %	80
Generator efficiency, %	98
DDGS dryer steam pressure, bar	9
Ethanol production steam pressure, bar	2.5
Deaerator pressure, bar	2
Solar field	
PTC concentrator length, m	150
PTC concentrator gross aperture width, m	5.76
PTC optical active aperture area factor, %	95
PTC row spacing, m	17.28
PTC peak optical efficiency, %	75
PTC mirror cleanliness factor, %	95

(1) relative to air stoichiometric; (2) relative to the total energy released in the combustion;

Table 3. Solar field design-point conditions

Parameters	**Phoenix/AZ (US)**	**Barreiras/BA (BR)**
Latitude	32.95	-12.14
Longitude	-111.77	-44.99
DNI(1), W/m^2	956	908
Ambient temperature(2), °C	22	24
Wind speed(2), m/s	2.51	3.15
Solar multiple	1	1
Day(3)	June 21st	December 22nd

(1) defined as 90% of the cumulative frequency distribution of the hourly non-null irradiance; (2) annual average; (3) at noon;

2.2 Modeling and simulation

The following simplifying assumptions are considered in the analysis:

1. Steady-state operation (in each hourly time step).
2. The heat exchangers are adiabatic and of counter-current type.
3. The heat losses caused by boiler purges are neglected.
4. All the flash steam generated is released into the atmosphere and is replaced as make-up water in the condensate tank.
5. At a 40% part-load regime, it is considered an excess air ratio of 60% and combustion chamber efficiency of 96%.
6. The pressure losses across the boiler and the solar field are equal and constant.
7. Kinetic and potential energy variations are neglected.
8. The reference ambient conditions are a temperature of 288.15 K and a pressure of 1 bar.
9. Ash chemical exergy is neglected.
10. All lost exergy is considered as destroyed exergy.

The mass, energy, and exergy balance are considered according to Eq. (1) to Eq. (3), respectively:

$$\sum \dot{m}_{in} = \sum \dot{m}_{out} \quad (1)$$

$$\dot{Q}_{in} + \dot{W}_{in} + \sum(\dot{m}h)_{in} = \dot{Q}_{out} + \dot{W}_{out} + \sum(\dot{m}h)_{out} \quad (2)$$

$$\dot{B}_{in} = \dot{B}_{out} + \dot{B}_{d} \quad (3)$$

Before the energy and exergy analysis, a last relevant parameter regarding the solar field area is defined as:

$$A_{SF,net} = \frac{0.6 \cdot \dot{Q}_{boiler,FL}}{(\dot{Q}_{SF,th} - \dot{Q}_{SF,loss}) \cdot SM} \cdot A_{PTC,net} \quad (4)$$

where $A_{SF,net}$ is the net aperture area covered by concentrators in the solar field, $\dot{Q}_{boiler,FL}$ is the energy flux delivered by the boiler at full-load, $\dot{Q}_{SF,th}$ is the thermal energy flux absorbed by the concentrators, $\dot{Q}_{SF,loss}$ is the thermal energy loss flux in the solar field, SM is the solar multiple, and $A_{PTC,net}$ is the net aperture area of a parabolic trough concentrator unit. The total net aperture area is calculated for each location using their respective design point conditions.

For the energy analysis, the boiler energy efficiency, solar field optical efficiency, and solar field thermal efficiency are calculated according to Eq. (5) to Eq. (8), respectively:

$$\eta_{boiler} = \frac{(\dot{m}_{30}h_{30}) - (\dot{m}_{29}h_{29})}{\dot{m}_{biomass,34} \cdot LHV} \quad (5)$$

$$\eta_{SF,optc} = \frac{\dot{Q}_{SF,th}}{DNI \cdot A_{SF,net}} \quad (6)$$

$$\eta_{SF,th} = \frac{(\dot{m}_{33}h_{33}) - (\dot{m}_{32}h_{32})}{\dot{Q}_{SF,th}} \quad (7)$$

$$\eta_{cycle} = \frac{\dot{Q}_{Dryer} + \dot{Q}_{eprod} + \dot{W}_{turb1} + \dot{W}_{turb2}}{(\dot{m}_{biomass,34} \cdot LHV) + (DNI \cdot A_{SF,net})} \quad (8)$$

In the previous equations, DNI is the direct normal irradiance that reaches the solar field, and LHV is the low heating value of the fuel. Thus, the biomass saved by introducing the solar field is given by:

$$\boldsymbol{FS = \int_0^{8760} \dot{m}_{biomass,base} dt - \int_0^{8760} \dot{m}_{biomass,hybrid}\, dt} \tag{9}$$

The solar fraction is the portion of the plant's thermal demand provided by the solar field and is calculated with:

$$\boldsymbol{Solfrac = \frac{FS}{\int_0^{8760} \dot{m}_{biomass,base} dt}} \tag{10}$$

The exergy contained in any matter flow in the cycle is considered in the analysis as follows:

$$\boldsymbol{b = b_{ph} + b_{ch}} \tag{11}$$

where the physical exergy is defined by

$$\boldsymbol{b_{ph} = h - h_0 - T_0(s - s_0)} \tag{12}$$

and the chemical exergy, here considered only for the fuel, according to Styrylska and Szargut's model (Szargut, 2005), is

$$\boldsymbol{b_{ch} = (LHV + 2257w)\beta + b_{ch,w}} \tag{13}$$

where w is the fuel moisture mass ratio. The parameter β is estimated by:

$$\boldsymbol{\beta = \frac{1.042 + 0.216\left(\frac{z_{H_2}}{z_C}\right) - 0.2499\left(\frac{z_{O_2}}{z_C}\right)\left[1 + 0.7884\left(\frac{z_{H_2}}{z_{O_2}}\right)\right] + 0.045\left(\frac{z_{N_2}}{z_C}\right)}{1 - 0.3035\left(\frac{z_{O_2}}{z_C}\right)}} \tag{14}$$

where z is the mass ratio of the elements in the fuel.

The solar exergy is calculated using the solar energy to exergy conversion ratio proposed by Spanner (Petela, 2003), Eq. (15).

$$\boldsymbol{\dot{B}_{solar} = DNI \cdot A_{SF,net} \cdot \left(1 - \frac{4}{3} \cdot \frac{T_0}{T_{solar}}\right)} \tag{15}$$

where T_{solar} is assumed equal to 5777 K.

The exergy destruction and exergetic efficiency for every component of the cogeneration cycle can be found in Table A.1 of Appendix A. Lastly, the energetic and exergetic analyses were performed using the EBSILON Professional software, version 14.03, and typical meteorological year data from Meteonorm.

3. RESULTS

Table 4 presents the results of the energy performance parameters concerning the base-case and hybrid-case scenarios of the power plant on their design-point condition. This means that the base case runs entirely on biomass combustion while the hybrid-cases are running under their specific design-point conditions, as presented in Table 3. Furthermore, the hybrid- cases results of Table 4 were found by determining the solar field size considering the design specifications that the solar field at design conditions generates a maximum of 60% of the total steam requirement and that the solar field loops are composed of 8 PTC concentrators each. Consequently, it was found that for Phoenix, the solar field must have 168 concentrators, totaling a net aperture area of 137328 m2, and for Barreiras the solar field must have 176 concentrators, accounting for a net aperture area of 143867 m2.

From Table 4, it can be noticed that at design conditions, there is a reduction of 57% e 60% of biomass consumption for Phoenix and Barreiras, respectively. Also, it can be noticed that for design conditions, the hybrid plant in both locations has nearly identical thermodynamic performance, as can be detected in the plants' efficiencies.

Table 5 presents the results of the exergy performance parameters of the base-case and hybrid-case scenarios. These results show that for all cases shown, the boiler and solar field represent together more than 91% of all destroyed exergy. Excluding the boiler and solar field feed pumps, all other components have similar exergy performance in all three cases. This behavior results from the plant being designed to run the industrial processes on a steady-state basis. Therefore, it is expected that the annual exergetic performance of most components will be equal to or similar to that of the design-point analysis.

Table 4. Energy performance parameters at the design point

Parameter	Base case	Hybrid case Phoenix/AZ (US)	Hybrid case Barreiras/BA (BR)
Biomass consumption, kg/s	13.3	5.5	5.5
Boiler steam production, kg/s	49	20	20
Solar field steam production, kg/s	0	29	29
Boiler biomass energy input, MWh	169	71	71
Concentrator incident solar energy, MWh	-	131	131
Solar field optical energy losses, MWh	-	40	40
Solar field thermal energy losses, MWh	-	6	6
DDGS dryer process heat consumption, MWh	25	25	25
Ethanol production process heat consumption, kWh	82	82	82
Plant electricity output, MWh	28.5	28	28
Plant electricity consumption, MWh	8	8	8
Boiler energy efficiency, %	85	83	83
Solar field optical efficiency, %	-	70	70
Solar field energy efficiency, %	-	94	93
Global energy efficiency, %	**80**	**68**	**68**

Table 5. Exergy performance parameters at the design point

Component	**Base-case**			**Hybrid-case Pheonix/AZ (US)**			**Hybrid-case Barreiras/BA (BR)**		
	Destroyed Exergy (kW)	Exergetic Efficiency (%)	Exergy Destruction Ratio (%)	Destroyed Exergy (kW)	Exergetic Efficiency (%)	Exergy Destruction Ratio (%)	Destroyed Exergy (kW)	Exergetic Efficiency (%)	Exergy Destruction Ratio (%)
Boiler	**127265**	**36**	**91.21**	**53920**	**35**	**37.48**	**52823**	35	**37.08**
Solar Field	**0**	-	-	**77667**	**36**	**54.0**	**79799**	35	**54,49**
Turbine 1	1587	93	1.14	1592	93	1.11	1593	93	1.10
Turbine 2	553	92	0.40	555	92	0.39	555	92	0.38
Piping 1	2721	92	1.95	2726	92	1.90	2727	92	1.88
Piping 2	279	98	0.20	280	98	0.19	280	98	0.19
Atemperator 1	170	99	0.12	147	99	0.10	141	99	0.10
Atemperator 2	166	99	0.12	153	99	0.11	150	99	0.10
DDGS Dryer	849	91		849	91	0.59	849	91	0.59
Ethanol Production Processes	3063	88	2.20	3063	88	2.13	3063	88	2.11
Steam trap 1	116	97	0.08	116	97	0.08	116	97	0.08
Steam trap 2	273	87	0.20	273	87	0.19	273	87	0.19
Condensate Tank	2268	58	1.63	2268	58	1.58	2268	58	1.57
Deaerator	141	98	0.10	139	98	0.10	139	98	0.09
Cond. Pump 1	1	85	0	1	85	0	1	85	0
Cond. Pump 2	0.4	86	0	0.4	86	0	0.4	86	0
Cond. Pump 3	68	86	0.05	25	86	0.02	25	86	0.02
Cond. Pump 4	0	-	-	41	86	0.03	41	86	0.03
Global	**139521**	**30**	**100**	**143814**	**30**	**100**	**144842**	**30**	**100**

The annual energy performance results are found in Table 6. It can be seen that the introduction of the solar field produceda biomass saving of 60145 tons for the plant located in Phoenix and 50871 tons for the plant located in Barreiras. These savings represent a solar fraction of 14.36% and 12,15%, respectively, which means that the plant in Phoenix ran the equivalent of 52.4 days of the year using solar energy while the plant in Barreiras ran for around 44.3 days.

Furthermore, the energy efficiencies of the annual analysis show the influence of the plant's location and environmental conditions. For example, the plant in Phoenix has a much worse optical performance than the plant situated in Barreiras,partially because it is above the Tropic of Cancer (23.43°). On the other hand, the hybrid plant located in Phoenix has a better annual solar field thermal efficiency than the plant situated in Barreiras, which can be associated with climatic conditions that favor fewer heat losses.

Concerning the exergetic analysis of the annual operation of the hybrid plant, it can be noted that the boiler and the solar field continue to account for around 91 % of the total exergy destroyed in all cases. However, the share of these components in exergy destruction changes. For Phoenix, the boiler exergy destruction contribution goes from 37.49 % in the design-point conditions to 73.39% in the annual analysis. In comparison, the solar field contribution to exergy destruction goes from 54% under design conditions to 18.39 % in the yearly analysis (see Fig. 2). For Barreiras, the same exergy destruction change happens with the boiler annual exergy destruction ratio going to 77.25% and the solar field's ratio to 14.29%. This change is the result of the low solar fraction. However, it is essential to notice that lower solar field

efficiency in Phoenix leads to a higher contribution of the solar field in the annual exergy destruction for this location and a lower yearly global exergy efficiency.

Table 6. Annual energy performance parameters

Parameter	Base plant	Hybrid case Phoenix/AZ (US)	Hybrid case Barreiras/BA (BR)
Total biomass consumed, t	**418703**	**358570**	**367844**
Boiler biomass energy input, GWh	1483	1344	1302
Concentrator incident solar energy, GWh	-	375	278
Solar field optical energy losses, GWh	-	241	101
Solar field's absorber and piping thermal energy loss, GWh	-	15	21
Solar field defocusing losses, GWh	-	0	1
Dryer process heat consumption, GWh	222	222	222
Ethanol production process heat consumption, GWh	717	717	717
Plant electricity output, GWh	249	249	249
Plant electricity consumption, GWh	70	70	70
Boiler energy efficiency, %	85	85	85
Solar field optical efficiency, %	-	58	64
Solar field energy efficiency, %	-	89	87
Global energy efficiency, %	**80**	**73**	**75**

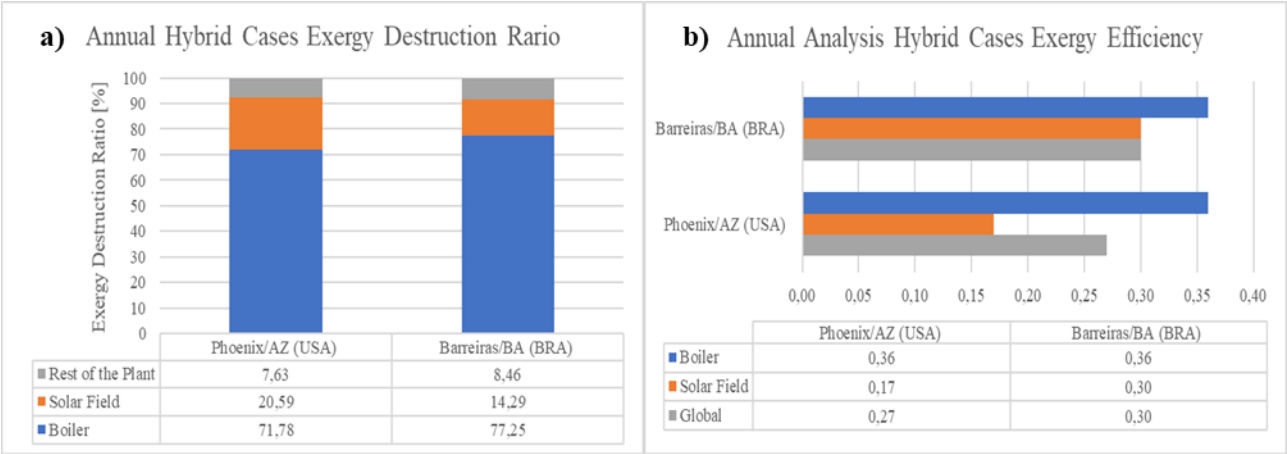

Fig. 2. Hybrid-cases annual exergetic analysis results: a) ratio of exergy destruction per component, b) exergy efficiency.

4. CONCLUSION

At the present work, a 28.5 MWe hybrid solar-biomass cogeneration power plant used by a 264,000 m^3/year corn ethanolplant was simulated for two locations: Phoenix/AZ (US) and Barreiras/BA (BR). The simulation performed covered the plant operation at design conditions and during an hourly typical meteorological year. The results show that the CSP technology's introduction presents relevant technical advantages over the biomass-only base case with better solar field performance in Barrreiras. For the Phoenix site, a total biomass saving of 60145 tons is obtained through the year, represents a solar fraction of 14.36 %, representing the equivalent of 52 days of biomass use. On the other hand, for the Barreiras site, 50871 tons of biomass were saved during the year resulting in a solar fraction of 12.15%, the equivalent of 44 days of biomass use. The exergetic analysis shows the boiler and the solar field accounting for more than 91% of the total exergy destruction of the plant in all cases analyzed; however, the proportion of the exergy destruction between theboiler and solar field changes from the design point to annual analysis. Due to the low solar fraction, the boiler of the hybrid-cases works most of the time though the year, leading to a yearly exergy destruction ratio larger than 70 % both in Phoenix and Barreiras. Both locations present, in general, similar results. The previously presented results show that a significant amount of fuel can be saved by introducing the CSP technology to the ethanol industry while maintaining good technical performance, indicating that the proposed solution is technically feasible for both locations studied. Nevertheless, to gauge the real prospects of implementation, it is necessary to perform a further financial evaluation.

ACKNOWLEDGMENTS

The authors acknowledge the Piracicaba Engenharia and SL Process companies for providing technical data, as well as the National Council for Scientific and Technological Development (CNPq), the Coordination for the Improvement of Higher Education Personnel (CAPES) and Araucaria Foundation (CP 20/2018 PPP - contract number 047/2020) for the financial support.

REFERENCES

Brunet, R., Guillén-Gosálbez, G. and Jiménez, L. (2014), "Minimization of the nonrenewable energy consumption in bioethanol production processes using a solar-assisted steam generation system", AIChE Journal, Vol. 60 No. 2, pp. 500–506.

Burin, E.K., Buranello, L., Lo Giudice, P., Vogel, T., Görner, K. and Bazzo, E. (2015), "Boosting power output of a sugarcane bagasse cogeneration plant using parabolic trough collectors in a feedwater heating scheme", Applied Energy, Vol. 154, pp. 232–241.

Cortez, L.A.B., Lora, E.E.S. and Gómez, E.O. (Eds.) (2008), Biomassa para energia, Unicamp, Campinas.

Donke, A.C.G., Matsuura, MISF, Sugawara, E.T., Kulay L. (2013), "Energo and Exergo-Environmental Analysis of a Multipurpose Process for Ethanol Production from Sugarcane and Corn", ELCAS3: Proceedings of the 3rd International Exergy, Life Cycle Assessment, and Sustainability Workshop & Symposium; Nisyros, Greece.

Eckert, C.T., Frigo, E.P., Albrecht, L.P., Albrecht, A.J.P., Christ, D., Santos, W.G., Berkembrock, E. and Egewarth, V.A. (2018), "Maize ethanol production in Brazil: Characteristics and perspectives", Renewable and Sustainable Energy Reviews, Vol. 82, pp. 3907–3912.

Fuqiang, W., Ziming, C., Jianyu, T., Yuan, Y., Yong, S. and Linhua, L. (2017), "Progress in concentrated solar power technology with parabolic trough collector system: A comprehensive review", Renewable and Sustainable Energy Reviews, Vol. 79, pp. 1314–1328.

Giglio, A., Lanzini, A., Leone, P., Rodríguez García, M.M. and Zarza Moya, E. (2017), "Direct steam generation in parabolic-trough collectors: A review about the technology and a thermo-economic analysis of a hybrid system", Renewable and Sustainable Energy Reviews, Vol. 74, pp. 453–473.

International Energy Association (IEA) (2019), World energy balances: Overview.

Kam, M.J. de, Morey, R.V. and Tiffany, D.G. (2009), "Integrating Biomass to Produce Heat and Power at Ethanol Plants", Applied Engineering in Agriculture, Vol. 25, pp. 227–244.

Karuppiah, R., Peschel, A., Grossmann, I.E., Martín, M., Martinson, W. and Zullo, L. (2008), "Energy optimization for the design of corn-based ethanol plants", AIChE Journal, Vol. 54 No. 6, pp. 1499–1525.

López J.C., Restrepo Á., Bazzo E. (2018). "Exergy Analysis of the Annual Operation of a Sugarcane Cogeneration Power Plant Assisted by Linear Fresnel Solar Collectors". ASME. Journal of Solar Energy Engineering; 140(6):061004.

Mani, S., Sokhansanj, S., Tagore, S. and Turhollow, A.F. (2010), "Techno-economic analysis of using corn stover to supply heat and power to a corn ethanol plant. Part 2: Cost of heat and power generation systems", Biomass and Bioenergy, Vol. 34 No. 3, pp. 356–364.

Morey, R.V., Tiffany, D.G. and Hatfield, D.L. (2006), "Biomass for Electrocity and Process Heat at Ethanol Plants", Applied Engineering in Agriculture, Vol. 22, pp. 723–728.

Nogueira, A.R., Donke, A.G., Matsuura, M.S.F.I., Matai, P.L.S.H. and Kulay, L. (2014), "Use of Environmental and Thermodynamic Indicators to Assess the Performance of an Integrated Process for Ethanol Production", Environment and Natural Resources Research, Vol. 4 No. 4.

Petela R. (2003), "Exergy of undiluted thermal radiation". Solar Energe. 74(6):469-88.

Renewable Fuels Association (RFA) (2019), 2019 Ethanol Industry Outlook.

Szargut J. (2005). Exergy method: Technical and ecological applications. Southampton, England: WIT Press.

Tiffany, D.G., Morey, R.V. and Kam, M.J. de, 2008. Use of Distillers By-Products and Corn Stover as Fuels for Ethanol Plants. *In Proceedings of Integration of Agricultural and Energy Systems Conference*. Atlanta, USA.

Wang, L., Hanna, M.A., Weller, C.L. and Jones, D.D., 2009, "Technical and economical analyses of combined heat and power generation from distillers grains and corn stover in ethanol plants", Energy Conversion and Management, Vol. 50 No. 7, pp. 1704–1713.

RESPONSIBILITY NOTICE

The authors are solely responsible for the printed material included in this paper.

APPENDIX A

Table A.1 contains the equations used to calculate the cogeneration cycle's destroyed exergy and exergetic efficiency and its components. The numbering of the exergy flows at Table A.1 follows the same order as indicated in Fig. 1.

Table A.1. Exergy destruction and exergetic efficient equations of the components and cycle

Component	Destroyed Exergy	Exergetic Efficiency
Boiler	$\dot{B}_{d,boiler} = \dot{B}_{comb} + \dot{B}_{27} - \dot{B}_{28}$	$\varepsilon_{boiler} = \frac{(\dot{B}_{27}-\dot{B}_{26})}{\dot{B}_{solar}}$
Solar Field	$\dot{B}_{d,SF} = \dot{B}_{solar} + \dot{B}_{30} - \dot{B}_{31}$	$\varepsilon_{SF} = \frac{(\dot{B}_{31}-\dot{B}_{30})}{\dot{B}_{solar}}$
Turbine 1	$\dot{B}_{d,turb1} = \dot{B}_1 + \dot{B}_2 - \dot{B}_{11} - \dot{W}_{turb1}$	$\varepsilon_{turb1} = \frac{\dot{W}_{turb1}}{(\dot{B}_1-\dot{B}_3-\dot{B}_{11})}$
Turbine 2	$\dot{B}_{d,turb2} = \dot{B}_2 + \dot{B}_3 - \dot{W}_{turb2}$	$\varepsilon_{turb2} = \frac{\dot{W}_{turb2}}{(\dot{B}_2-\dot{B}_3)}$
Piping 1	$\dot{B}_{d,pipe1} = \dot{B}_3 - \dot{B}_4$	$\varepsilon_{pipe1} = 1 - \left(\frac{\dot{B}_{d,pipe1}}{\dot{B}_3}\right)$
Piping 2	$\dot{B}_{d,pipe2} = \dot{B}_{11} - \dot{B}_{12}$	$\varepsilon_{pipe2} = 1 - \left(\frac{\dot{B}_{d,pipe2}}{\dot{B}_{11}}\right)$
Atemperator 1	$\dot{B}_{d,winjet1} = \dot{B}_5 + \dot{B}_{24} - \dot{B}_6$	$\varepsilon_{winjet1} = 1 - \left[\frac{\dot{B}_{d,winjet1}}{(\dot{B}_5+\dot{B}_{24})}\right]$
Atemperator 2	$\dot{B}_{d,winjet2} = \dot{B}_{12} + \dot{B}_{23} - \dot{B}_{13}$	$\varepsilon_{winjet2} = 1 - \left[\frac{\dot{B}_{d,winjet2}}{(\dot{B}_{12}+\dot{B}_{23})}\right]$
DDGS Dryer	$\dot{B}_{d,dryer} = \dot{B}_{13} + \dot{B}_{14} - \dot{B}_{th,dryer}$	$\varepsilon_{dryer} = \frac{\dot{B}_{th,dryer}}{(\dot{B}_{13}-\dot{B}_{14})}$
Ethanol Production Processes	$\dot{B}_{d,eprod} = \dot{B}_6 + \dot{B}_7 - \dot{B}_{th,eprod}$	$\varepsilon_{eprod} = \frac{\dot{B}_{th,eprod}}{(\dot{B}_6-\dot{B}_7)}$
Steam Trap 1	$\dot{B}_{d,strap1} = \dot{B}_7 - \dot{B}_8$	$\varepsilon_{strap1} = 1 - \left(\frac{\dot{B}_{d,strap1}}{\dot{B}_8}\right)$
Steam Trap 2	$\dot{B}_{d,strap2} = \dot{B}_{14} - \dot{B}_{15}$	$\varepsilon_{strap2} = 1 - \left(\frac{\dot{B}_{d,strap2}}{\dot{B}_{14}}\right)$
Condensate Tank	$\dot{B}_{d,ctank} = \dot{B}_{16} + \dot{B}_{17} - \dot{B}_{18}$	$\varepsilon_{ctank} = 1 - \left[\frac{\dot{B}_{d,ctank}}{(\dot{B}_{16}+\dot{B}_{17})}\right]$
Deaerator	$\dot{B}_{d,desea} = \dot{B}_9 + \dot{B}_{19} - \dot{B}_{20}$	$\varepsilon_{desae} = 1 - \left[\frac{\dot{B}_{d,desae}}{(\dot{B}_9-\dot{B}_{19})}\right]$
Condensate Pump 1	$\dot{B}_{d,pump1} = \dot{B}_{18} + \dot{W}_{pump1} - \dot{B}_{19}$	$\varepsilon_{pump4} = \frac{(\dot{B}_{19}-\dot{B}_{18})}{\dot{W}_{pump1}}$
Condensate Pump 2	$\dot{B}_{d,pump2} = \dot{B}_{21} + \dot{W}_{pump2} - \dot{B}_{22}$	$\varepsilon_{pump4} = \frac{(\dot{B}_{22}-\dot{B}_{21})}{\dot{W}_{pump2}}$
Condensate Pump 3	$\dot{B}_{d,pump3} = \dot{B}_{26} + \dot{W}_{pump3} - \dot{B}_{27}$	$\varepsilon_{pump4} = \frac{(\dot{B}_{27}-\dot{B}_{26})}{\dot{W}_{pump3}}$
Condensate Pump 4	$\dot{B}_{d,pump4} = \dot{B}_{29} + \dot{W}_{pump4} - \dot{B}_{30}$	$\varepsilon_{pump4} = \frac{(\dot{B}_{30}-\dot{B}_{29})}{\dot{W}_{pump4}}$
Cycle	$\dot{B}_{d,cycle} = \sum \dot{B}_d$	$\varepsilon_{cycle} = \frac{\dot{W}_{turb1}+\dot{W}_{turb2}+\dot{B}_{th,eprod}+\dot{B}_{th,dryer}}{\dot{B}_{biomass,34}+\dot{B}_{solar}+\dot{W}_{pump1}+\dot{W}_{pump2}+\dot{W}_{pump3}+\dot{W}_{pump4}}$